

Analysis and Modeling of AC and DC Micro-Grids for Prosumer Based Implementation

A. Samrat, B. Mehta*, S. Joshi

Department of Electrical Engineering, School of Technology, Pandit Deendayal Petroleum University, Gandhinagar, Gujarat, India

Abstract- In view of global targets to expurgate the carbon foot prints, presently major focus is on integrating prosumer renewable energy sources (RES). This has caught more interest in studying the impacts of AC and DC micro grid. Looking at the advantages of power transformers for stepping up and down the voltages, AC grids seem favorable for transmitting power over long distances, but AC grids are also often subjected to difficulties associated with them such as frequency dip, voltage drop due to line impedance, skin effect and Ferranti effect etc. Most of the sources and loads, particularly the renewables like solar, battery etc., in a micro grid are basically DC in nature and their operating voltages are low. Considering the conversion losses and transformer cost combined with problems of AC grid, DC micro grids are catching attention and their analysis is thus required. This paper presents the controls of various types of distributed generation sources (DGs) including renewable energy sources (RES) so as to integrate them to form a micro-grid. The AC and DC micro-grid models have been developed and its performance is assessed. Stability analysis is performed on both AC and DC micro-grid during permanent faults, temporary faults and sudden load variations to have a comparative outcome for selection of a better micro-grid.

Keyword: AC micro-grid, Converter control, DC micro-grid, Renewable Energy Sources.

1. INTRODUCTION

Due to substantial influence of technology, there is a continuous advancement in terms of time and scale of output in the way day to day activities are carried out. As things or tasks are required to be accomplished within time limit and with larger output volume, the scope of machines has increased. This has led to the growth of electricity demand. Sustainable growth is required for stability and to that respect using imperishable source of energy is the current need. Imperishable sources of energy involve renewable energy sources (RES) such as solar, wind, hydro, tidal etc. In order to harness these RES efficiently and effectively there are modern systems developed such as micro-grids. They convert the energy from RES to electricity which can be utilized as per requirement. The building of micro-grids not only provides the flexibility to utilize the electrical power optimally and economically but it also serves the purpose of reliability by minimize the severities caused by power blackouts. It

ensures continuous power to critical loads by generating power at the distribution facilities. The micro-grid can provide benefits to the utility by sharing power to reduce the peak loads and therefore it helps in maintaining stability [1]. Micro-grid might also help to reduce the transmission losses by producing power at distributed level using prosumer renewable energy sources which attracts a normal consumer to have more control and involvement.

In the literatures, discussion on the stability aspects of remote and utility connected micro grids depending on the modes of operation, control topology, types of micro sources and network parameters is given [2]. An organized way to plan the micro source operation, micro grid controller design, islanding procedure, frequency control and the load shedding criteria is also being given [2]. The frequency stability was explored when the motor starts and its load power changes, and faults of different types and at different locations occur [3]. An overview study about micro grid structures and control techniques was carried out focusing mainly on grid-forming, grid-feeding, and grid-supporting configurations [4]. A micro-grid model was analyzed including a mix of synchronous and inverter-based DGs with a combination of passive RLC and induction motor (IM) loads where it was observed that in the

Received: 25 Jul. 2020

Revised: 02 Nov. 2020

Accepted: 06 Nov. 2020

*Corresponding author:

E-mail: bhinal.mehta@sot.pdpu.ac.in (B. Mehta)

Digital object identifier: 10.22098/joape.2021.7515.1536

Research Paper

© 2021 University of Mohaghegh Ardabili. All rights reserved.

presence of IM loads, the micro grid may lose its stable operation even if the fault is isolated within a typical clearing time [5]. An enhanced control strategy for electronically coupled distributed energy resources that improves the performance of the host micro grid under network faults and transient disturbances was also done [6]. Studies involving Big Bang-Big Crunch (BB-BC) and Hybrid BB-BC algorithms for continuous adjustments in gains of proportional integral (PI) controllers for controlling voltage and frequency of the system was done [7, 8]. Advantage of dynamic control for PI controllers' gains is that the system is made more reliable and resilient in contingencies. For the control of frequency and voltage of an islanded mini / micro grid, use of reinforcement learning method (RL) was done, which is based on Markov decision process (MDPs). Advantage of RL method is that it has better dynamic response compared to the traditional PID controller for damping the voltage and frequency oscillations [9]. The main disadvantage of RL method is that it requires lot of previous data and computational capabilities which can diminish the results. For finding the optimal size of energy storage systems (ESS) in which microgrid investment cost as well as operating cost are minimized the combination of demand response program (DRP) and mixed integer programming (MIP) was used. The advantage of MIP is that reliability increases and there is 1.77 % reduction of total cost. Also, the use of DRP leads to 16.59 % reduction of total cost [10]. The disadvantages of DRP include lack of experience and the consequent need to employ extensive assumptions while modelling and evaluating. The study involving simultaneous operation of various energy sources consisting of micro combined heat and power sources (CHP), photovoltaic (PV) arrays, ESS etc. in grid-connected mode leads to better performance of the multicarrier microgrid (MCMG). The advantage of simultaneous operation of multiple energy infrastructures in MCMG is to reduce the total operation cost of future networks as compared with individual energy source operation [11]. The disadvantage of MCMG is that the central level regulation less and the complexity of the total system in event of contingency is huge.

The objective of the paper is to model and analyse the RES based AC micro grid and DC microgrid having modified converter control strategies in simple manner. The main motive of this work is to ascertain the type of micro-grid that will be more suitable for prosumer based RES in distribution side generation. At the start, explanation about the different converter

control strategies used in AC and DC micro-grids for control of power converters is discussed. In the subsequent sections the AC and DC micro-grid modelling has been explained with the rating of RES used. There are results being shown with their brief discussion for AC and DC micro-grid comparison. The performance of the proposed test systems and control strategy are verified by conducting various simulations in MATLAB/ SIMULINK. This study tries to address all the shortcomings in the literature survey in an easy manner.

2. CONVERTER CONTROL STRATEGIES USED IN THE MICRO-GRID

Power Electronic converters are required to be connected between the some DGs and the PCC to match the DG side parameters to PCC side parameters. In order to cater the load requirement, an efficient control over the converter output is required to maintain micro-grid stability. The main control parameters of the converter output in AC micro-grid are voltage, frequency, active power and reactive power while that in DC micro-grid are voltage and power. Different control strategies are used to control these parameters depending upon DG type and nature of micro-grid i.e. AC or DC. In AC micro-grid the control used are: Voltage and Frequency control (V and f control) and Active and Reactive power control (PQ control). In DC micro-grid the control used are: Rectifier control (AC-DC control) and Chopper control (DC-DC control).

Pulse Width Modulation (PWM) switching technique is used to control the switch operation in almost all the converters. A control signal is compared with the periodic and repetitive triangular or saw-tooth waveform. The frequency of the triangular waveform is considered f_s which serves as a switching frequency of the converter. If the control signal is greater than the triangular signal, a switching signal is generated to turn on the switch. Otherwise, switch will be in off condition. The control signal decides the shape of the output waveform and has frequency f_1 [12]

$$ma = \frac{V_{control}}{V_{tri}} \quad (1)$$

$$mf = \frac{f_s}{f_1} \quad (2)$$

Amplitude modulation ma is defined as the ratio of peak amplitude of the control signal to the peak amplitude of the triangular signal. For linear operation of the converter the range of ma is 0 to 1. Frequency modulation mf is defined as the ratio of switching frequency to the fundamental frequency [12].

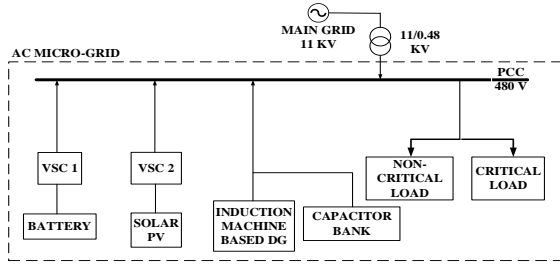


Fig. 1. Block diagram of AC Micro-grid test system

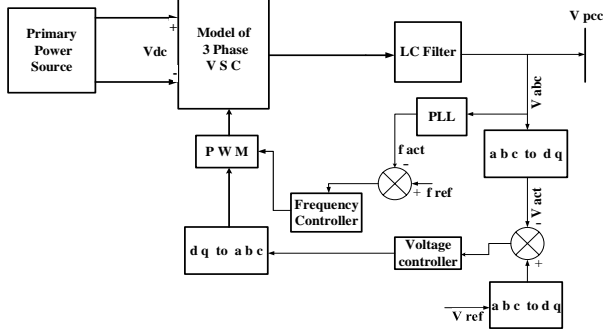


Fig. 2. PWM V and f control strategy [14]

3. MICRO-GRID MODELLING

3.1. Modelling AC micro-grid

As shown in Fig. 1, the main grid is modeled using a three phase voltage source with nominal rms line voltage of 11KV. The battery is modeled for a nominal voltage of 2000 V with 200 Ah capacity and 40 A nominal discharge current. The type of rotor for the induction generator is squirrel cage with an operating voltage of 480 Vrms. The operating frequency is at 50 Hz with a mechanical speed input. The solar panel is modeled using the SunPower SPR-305-WHT with 30 series connected modules and 66 strings connected in parallel [13]. The VSCs and their controls are modelled for having the grid supporting, feeding and forming capabilities.

The Non-critical and critical loads are modelled as an R-L-C load using RLC load block which draw the Active and Reactive power from PCC at nominal line voltage and frequency of 480 V, 50 Hz respectively. The capacitor bank for induction generator is also modelled using RLC block in library. For making and breaking the connections, three phase circuit breaker block is used with switching time. The three phase fault block is used with switching time for creation and completion of faults. The line impedance is modelled using the three phase PI section block.

3.1.1. Voltage and frequency control

According to Fig. 2, converter switches are controlled so that output voltage and frequency of the converter are equal to the reference voltage and frequency of the system [14]. This type of control can be used only if the

DG is capable of delivering power as and when required by load i.e. as the load increases the DG should be capable of catering the increase in power immediately. Park transformation (abc to dq0 transformation) is applied on both measured and reference voltage signals. After Park transformation the difference is sent to the voltage controller. Reverse park transformation (dq0 to abc) is applied to the output control signal from voltage controller and the transformed control signal fed as an input to the PWM generator which gives triggering signals to the converter switches. Also the frequency output is compared with reference and the frequency controller gives output signal to the PWM.

3.1.2 Active and reactive power control (PQ control)

In PQ feedback control technique, converter switches are controlled so that the output active and reactive power through the converter are equal to the reference active and reactive power set by the user. This type of control technique is used when distributed source can only provide fixed amount of power to the system.

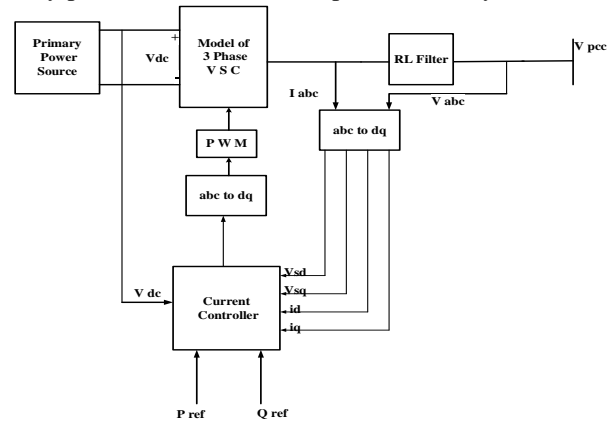


Fig. 3. PQ control technique [15]

As shown in Fig. 3, Park’s transformation is used to convert the three-phase voltages and currents at the PCC into dq components. The currents in the rotating reference frame i.e. i_d and i_q are proportional to the active and reactive power [15]. As the reference frame is synchronized with the PCC voltage, the quadrature voltage component, $V_{sq}=0$ and hence the power equations at the PCC can be written as [15]:

$$P_s = V_{sd}i_d \tag{3}$$

$$Q_s = -V_{sd}i_q \tag{4}$$

From equations (3) and (4) the reference currents for a current controlled inverter with predetermined power settings, P_{sref} and Q_{sref} are given by [15]:

$$i_{dref} = \frac{P_{sref}}{V_{sd}} \tag{5}$$

$$i_{qref} = \frac{-Q_{sref}}{V_{sd}} \tag{6}$$

The output control signal of current controller after reverse park transformation conversion is used as input

for PWM generator which gives triggering signals to the converter switches.

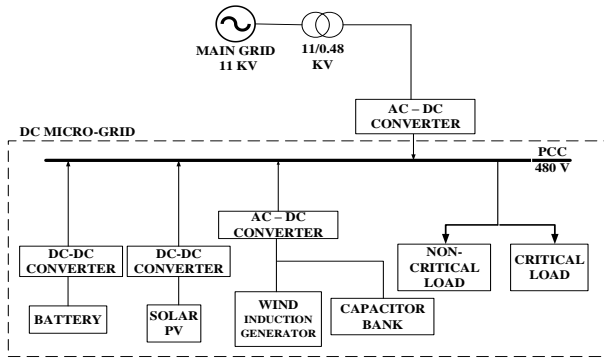


Fig. 4. DC micro-grid test system

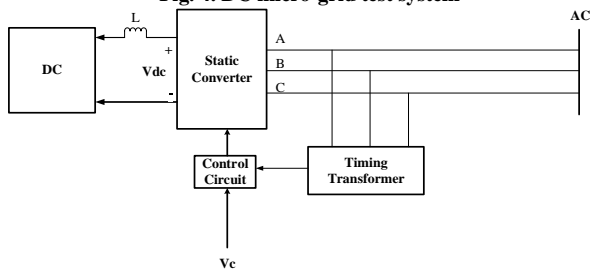


Fig. 5. Functional circuit blocks of a AC-DC converter [16]

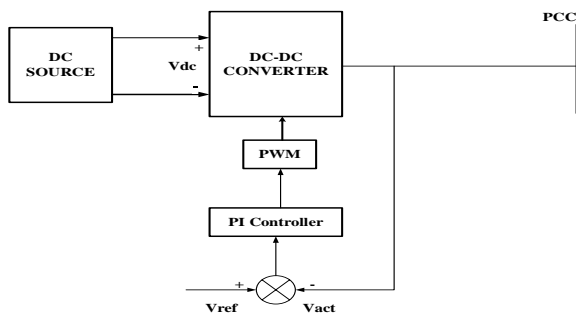


Fig. 6. PWM based control of DC-DC converter [17]

3.2. Modelling DC micro-grid

Fig. 4 depicts the block diagram for DC Micro-grid for 480 V PCC for its comparison with AC Micro-grid. The Main grid is interfaced with the PCC through a step-down transformer and AC-DC converters. The Battery based and Solar PV based DGs are connected to the PCC through DC-DC converters. The Induction machine based DG is connected to PCC via AC-DC converters. There is a capacitor bank connected with Induction machine based DG to supply it with reactive power requirements.

There are two types of loads connected in the DC Micro-grid i.e. Non-critical and Critical load. The Non-critical load is less important in nature as it can be sacrificed for some amount of time. Critical loads are to be catered all the time and can never be disconnected from the PCC. At the occurrence of any type of fault on the Main grid and distribution side, the Non-critical load gets disconnected and reconnects only when the fault is

cleared. The Critical load remains connected even during the fault.

3.2.1. Rectifier control (AC-DC control)

As per Fig. 5, connections at the AC terminals are labelled as A, B and C. The circuit block labelled static converter (SC) contains the switching elements. The control circuit block (CC) provides the switching pulses to the switches inside SC. The CC is designed to make the switching pulses adjustable. The adjustment is made by means of a control voltage, labelled V_c . The CC also needs timing inputs from the AC supply, because it has to have the reference instants in every AC cycle with respect to which the switching pulses delays are to be implemented. The timing reference instants are obtained from the timing transformer block, labelled TT in the figure. There are three small transformers in this block. This block TT provides a low voltage replica of the input AC waveform to the CC. Like all electronic signal processing circuits, the CC may need low voltage regulated DC power. This is not shown in the figure. If the AC-DC converter is an uncontrolled rectifier, in which all the switching elements are diodes, the timing transformer block and the control circuit block are not there. A filter is used to bring this ripple component down within acceptable limits. The filter element used for higher power applications is inductor, labelled as L in the Fig.5

3.2.2. Chopper control (DC-DC control)

As per Fig.6, DC-DC converter in closed loop control is used to convert the voltage levels as required at PCC from DC source DGs. The PI controller helps DC-DC converter to maintain reference output voltage. The PWM sets the switching of switches inside the DC-DC converter [17]. Thus, the study for PCC Voltage, Grid side Voltage and Current and Power catering by all the DG sources is done.

4. RESULTS AND DISCUSSION

Different contingencies can be studied upon the AC and DC Micro-grid. Here, majorly three situations have been studied namely:

Case 1: Stability of micro-grid at three phase fault on main-grid.

Case 2: Stability of micro-grid at sudden loading.

Case 3: Stability of micro-grid at temporary fault on main-grid.

The detailed results and discussion of all cases are given below.

Case 1: Stability Analysis of micro-grid when a three phase fault occurred on main grid

As a sudden three phase fault occurs at main grid at $t=10s$, immediately the micro-grid operates in islanded mode and disconnects from the grid. The non-critical loads are disconnected to ensure that the micro-grid cater power only to critical loads. Table 1 and Table 2 show the load change before and after the fault in AC and DC micro-grid.

Table 1. Load on AC micro grid before and after fault

Fault status	Active Load	Reactive Load
Before fault	500 KW	67 KVAR
After fault	160 KW	42 KVAR

Table 2. Load on DC micro-grid before and after fault

Fault status	Load
Before fault	500 KW
After fault	195 KW

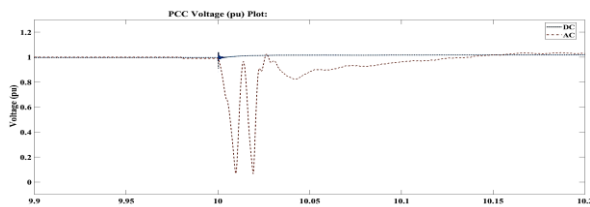


Fig. 7.1. Voltage response at point of common coupling (PCC)

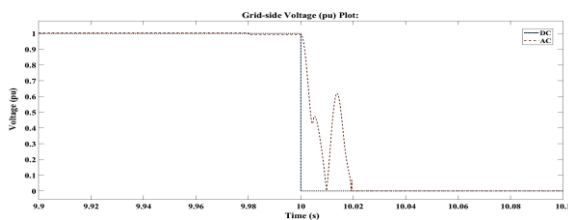


Fig. 7.2 Main grid voltage response

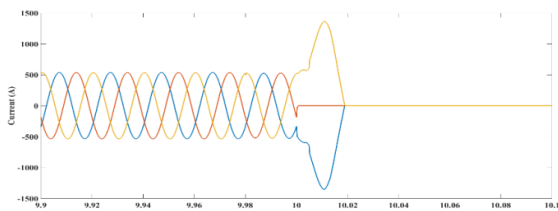


Fig. 7.3. Current from Main-grid in AC micro-grid

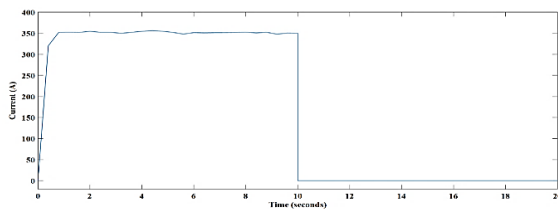


Fig. 7.4. Current from Main-grid in DC micro-grid

As per Fig. 7, the PCC and main-grid voltage plots and current waveform plots show the comparison of AC and DC micro-grid during the three phase fault at main-grid side. In Fig.7.1, it can be observed that just after the fault initiation and before islanding, there is large distortion in

the magnitudes of voltage and current in case of AC micro-grid as compared to DC micro-grid. The current from AC main grid spikes to 1400A from 500A before going to 0. Also the distortions last longer i.e. 10s to 10.02s in AC micro-grid as compared to DC micro-grid. As per Fig.7.3 &7.4, it is observed that current from main grid falls to zero as the main grid gets disconnected.

Case 2: Stability Analysis of micro-grid during sudden load variations in grid connected mode

A sudden load is applied to the micro-grid at $t= 10$. Immediately the excess load is shared among the sources to maintain stability of the system by balancing power demand with power generated. Table 3 and Table 4 show the load change before and after the sudden load variation in AC and DC micro-grid.

Table 3. Load on AC micro-grid before and after the sudden load variation

Status	Active Load	Reactive Load
Before adding sudden load	440 KW	57.5 KVAR
After adding sudden load	500 KW	67 KVAR

Table 4. Load on DC micro-grid before and after load variations

Status	Load
Before adding sudden load	440 KW
After adding sudden load	500 KW

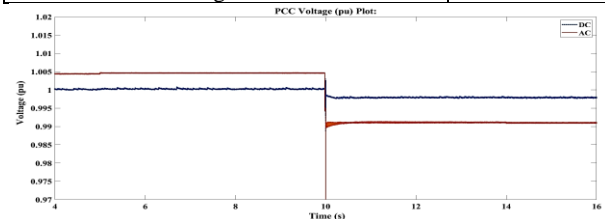


Fig. 8.1. Voltage response at Point of common coupling (PCC)

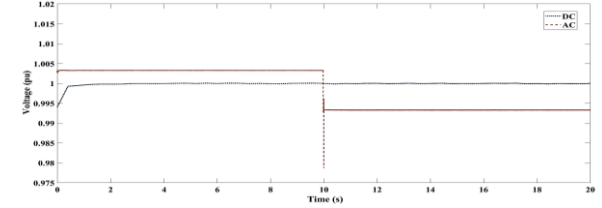


Fig. 8.2. Main grid Voltage response

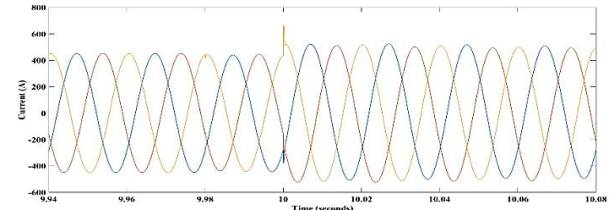


Fig. 8.3. Current from Main-grid in AC micro-grid

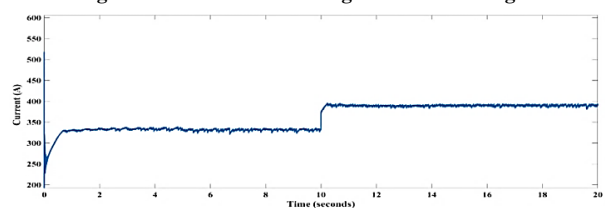


Fig. 8.4. Current from Main-grid in DC micro-grid

As per Fig. 8, the PCC and main-grid voltage plots and current waveform plots show the comparison of AC and DC micro-grid during the sudden load variation. As per Fig.8.3 & 8.4, it can be observed that just after the sudden load addition, there is more spike i.e. 420A to 700A in the magnitude of current in case of AC micro-grid as compared to DC micro-grid i.e 330A to 380A. Also, AC micro-grid seems more impacted as compared to DC micro-grid in terms of PCC and main-grid voltage magnitudes as in AC micro-grid, voltage drop is significant comparatively.

Case 3: Stability Analysis of AC micro-grid during temporary fault on main grid

The main grid suffers from a temporary fault at t=10s. During the fault time, the micro-grid enters into islanded mode by disconnecting non-critical loads from it. Immediately after the fault is cleared, the micro-grid operates in grid connected mode providing power to load along with the main grid. Table 5 and Table 6 show the load change before, during and after the temporary fault in AC and DC micro-grid.

Table 5. Load on AC micro-grid before, during and after the temporary fault

Fault status	Active Load	Reactive Load
Before fault	500 KW	67 KVAR
During fault	160 KW	42 KVAR
After fault	500 KW	67 KVAR

Table 6. Load on DC micro-grid before, during and after temporary fault

Fault status	Load
Before fault	500 KW
During fault	195 KW
After fault	500 KW

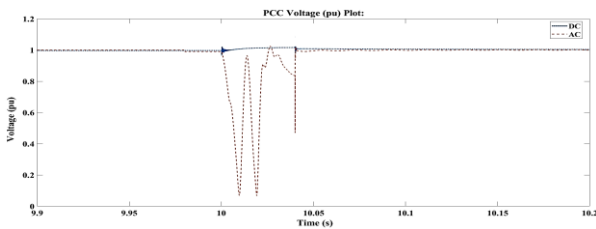


Fig. 9.1. Voltage response at Point of common coupling (PCC)

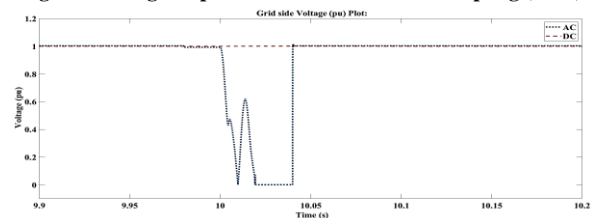


Fig. 9.2. Main grid Voltage response

As per Fig. 9, the PCC and main-grid voltage plots and current waveform plots show the comparison of AC and DC micro-grid before, during and after the sudden load variation on micro-grid side.

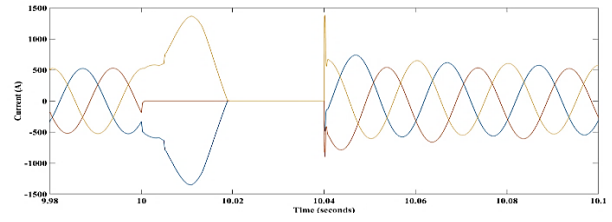


Fig. 9.3. Current from Main-grid in AC micro-grid

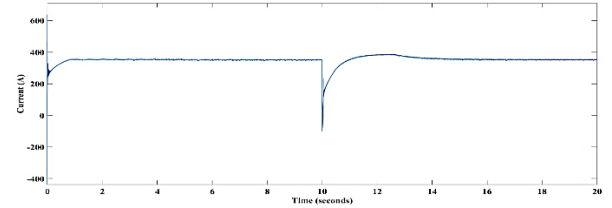


Fig. 9.4. Current from Main-grid in DC micro-grid

It can be observed that just after the fault initiation and before islanding, there is large distortion in the magnitudes current in case of AC micro-grid i.e. 500A to 1400A as compared to DC micro-grid i.e 300A to 350A. Also the voltage dip is larger in AC micro-grid when the reconnection occurs after the temporary fault gets cleared and main-grid gets reconnected.

5. CONCLUSIONS

In comparison with DC micro grid in AC micro grid the voltage drop of the line depends not only on resistive drop but also on reactive drop. This characteristics of AC system in AC microgrid is proved in the simulation and clearly depicts that voltage and current ripple in the line in AC system will be more than that of DC system. Results indicate that DC micro-grid attains stability faster than the AC micro-grid immediately as a fault gets cleared. Control for the converters in the DC system are simple as they do not need to have control over the frequency of the converter output signal. Comparitvie anlaysis is sucessfully carred out for AC and DC Microgrid for analysing the stability during the different types of disturbances like three phase fault, suddent change in load and temporary fault. In all three cases under consideration DC micro grid gains advatnages compared to AC microgrid. Practically the DC micro-grid systems do not suffer from skin effect or Ferranti effect. Advantages of the DC micro-grid system might play an important role in the future to make a transition from AC to DC micro-grid systems at distribution side prosumer based RES applications.

Appendix A

Table I. Ratings of Battery

Type of battery	Nominal Voltage	Nominal Discharge Current	Maximum Capacity
Nickel-Metal Hydride	2000 V	40 A	215 Ah

Table II. Ratings of Induction Generator

Type of rotor	Operating Voltage	Frequency of operation	No of pole pairs
Squirrel cage	480 V (ph-ph)	50 Hz	2

Table III. Rating of Solar PV

Module Voltage at STC	Module Current at STC	Total Voltage at maximum power point	Total Current from maximum power point
54.7 V	5.58 A	1641 V	368 A

REFERENCES

- [1] N. Hatziaargyriou, A. Anastasiadis, J. Vasiljevska and A. Tsikalakis, "Quantification of economic, environmental and operational benefits of microgrids", *Power Tech. Conf.*, 2009.
- [2] R. Majumder, "Some aspects of stability in microgrids", *IEEE Trans. Power Syst.*, vol. 28, pp. 3243-52, 2013.
- [3] X. Zhao-Xia and F. Hong-Wei, "Impacts of P-f and Q-V droop control on micro grids transient stability", *Phys. Procedia.*, vol. 24. Pp. 276-82, 2012.
- [4] J. Rocabert, A. Luna, F. Blaabjerg and P. Rodríguez, "Control of power converters in AC microgrids", *IEEE Trans. Power Electron.*, vol. 27, pp. 4734-49, 2012.
- [5] A. Alaboudy, H. Zeineldin and J. Kirtley, "Microgrid stability characterization subsequent to fault-triggered islanding incidents", *IEEE Trans. Power Delivery*, vol. 27, pp. 658-69, 2012.
- [6] M. Zamani, A. Yazdani and T. Sidhu, "A control strategy for enhanced operation of inverter-based microgrids under transient disturbances and network faults", *IEEE Trans. Power Delivery*, vol. 27, pp. 1737-47, 2012.
- [7] A. Moarref, M. Sedighzadeh and M. Esmaili, "Multi-objective voltage and frequency regulation in autonomous microgrids using pareto-based big bang-big crunch algorithm", *Control Eng. Pract.*, vol. 55, pp. 56-68, 2016.
- [8] M. Sedighzadeh, M. Esmaili and A. Moarref, "Voltage and frequency regulation in autonomous microgrids using hybrid big bang-big crunch algorithm", *Appl. Soft Comput.*, vol. 52, pp. 176-89, 2017.
- [9] H. Shayeghi and A. Younesi, "Mini/micro-grid adaptive voltage and frequency stability enhancement", *J. Oper. Autom. Power Eng.*, vol. 7, pp. 107-18, 2019.
- [10] M. Majidi and S. Nojavan, "Optimal sizing of energy storage system in a renewable-based microgrid under flexible demand side management considering reliability and uncertainties", *J. Oper. Autom. Power Eng.*, vol. 5, pp. 205-14, 2017.
- [11] V. Amir, S. Jadid and M. Ehsan, "Operation of multi carrier microgrid (MCMG) considering demand response", *J. Oper. Autom. Power Eng.*, vol. 7, pp. 119-28, 2019.
- [12] M. Ned, M. Udeland and P. Robbins, "Switch-mode DC-AC inverters: DC to sinusoidal AC", *Power Electron. Converters Appl. Des.*, 3rd edition, 2003.
- [13] Z. Salam, K. Ishaque and H. Taheri, "An improved two-diode photovoltaic (PV) model for PV system", *Power Electron. Drives Energy Syst. Int. Conf.* 2010.
- [14] Y. Wang, Z. Lu, Y. Min and S. Shi, "Comparison of the voltage and frequency control schemes for voltage source converter in autonomous microgrid", *2nd IEEE Int. Symp. Power Electron. Distrib. Gener. Syst.*, 2010.
- [15] M. Chamana and S. Bayne, "Modeling and control of directly connected and inverter interfaced sources in a microgrid", *IEEE North Am. Power Symp.*, 2011.
- [16] J. Vithayathil, "Line commutated converters", *Power Electron. Principles Appl.*, 10th reprint, 2016.
- [17] M. Ned, T. Udeland and W. Robbins, "DC-DC Switch mode converters", *Power Electron. Converters Appl. Design*, 3rd edition, 2003.